

Supporting Information

Novel porous molybdenum tungsten phosphide hybrid nanosheets on carbon cloth for efficient hydrogen evolution

Xu-Dong Wang, Yang-Fan Xu, Hua-Shang Rao, Wei-Jian Xu, Hong-Yan Chen, Wei-Xiong Zhang, Dai-Bin Kuang* and Cheng-Yong Su

MOE Key Laboratory of Bioinorganic and Synthetic Chemistry, Lehn Institute of Functional Materials, School of Chemistry and Chemical Engineering Sun Yat-sen University, Guangzhou 510275, P. R. China.

* Corresponding author. E-mail address: kuangdb@mail.sysu.edu.cn.

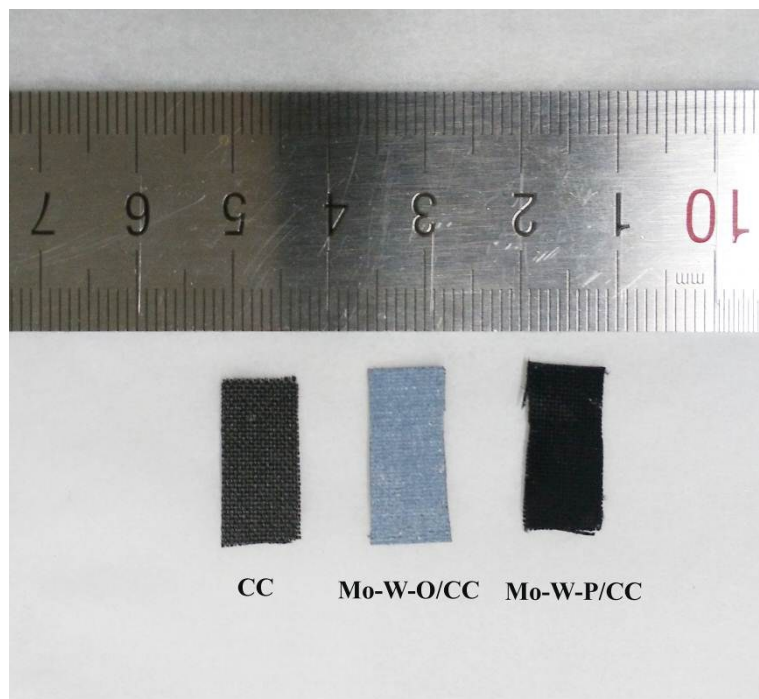


Fig. S1 Photograph of blank CC (left), Mo-W-O NWs/CC (middle), and Mo-W-P NSs/CF (right).

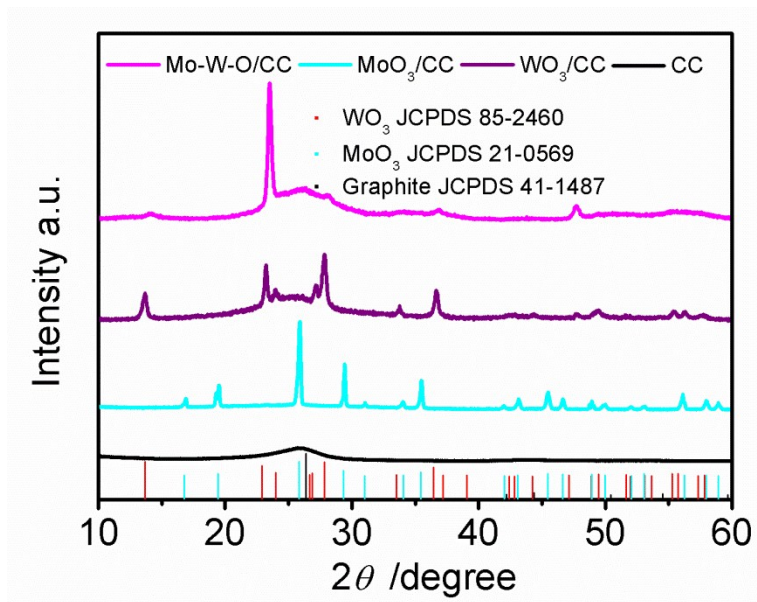


Fig. S2 The XRD patterns of Mo-W-O/CC, MoO₃/CC, WO₃/CC and CC.

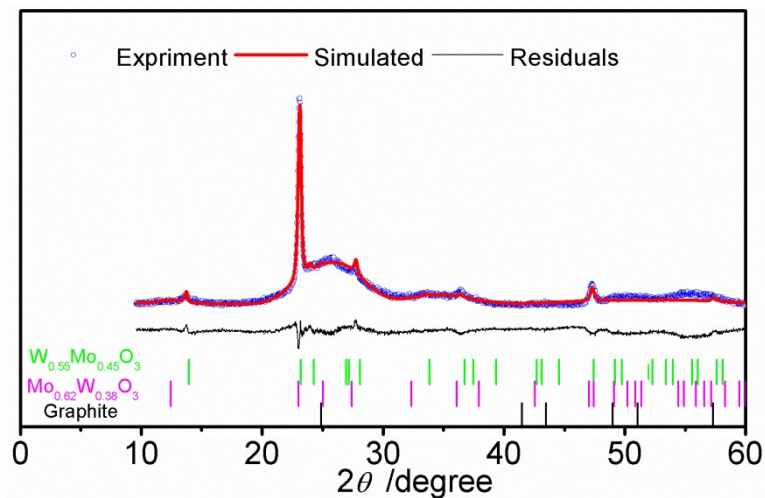


Fig.S3 The XRD patterns of the Mo-W-O analyzed by the Rietveld process. The positions of the peaks belonging to the phases used in the Rietveld fit of each spectrum are indicated with vertical markers.

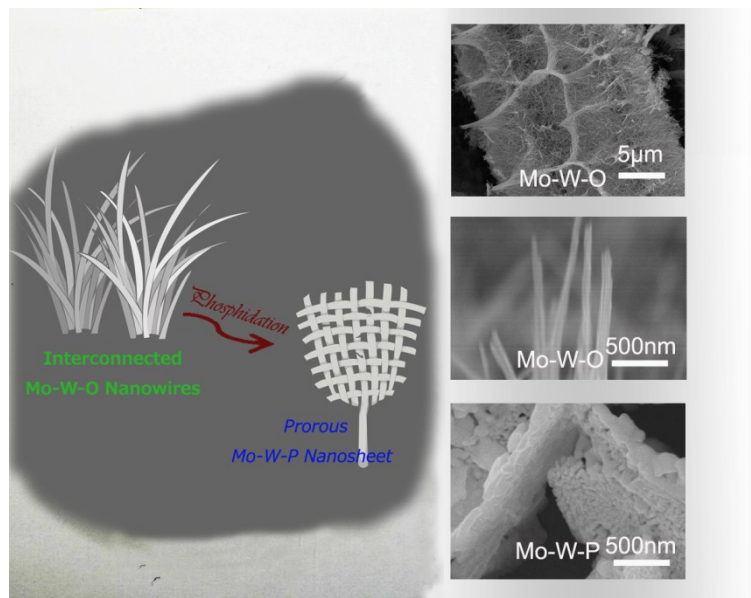


Fig. S4 Schematic illustration of the integration process of interconnected Mo-W-O hybrid nanowires to porous Mo-W-P nanosheets after phosphidation.

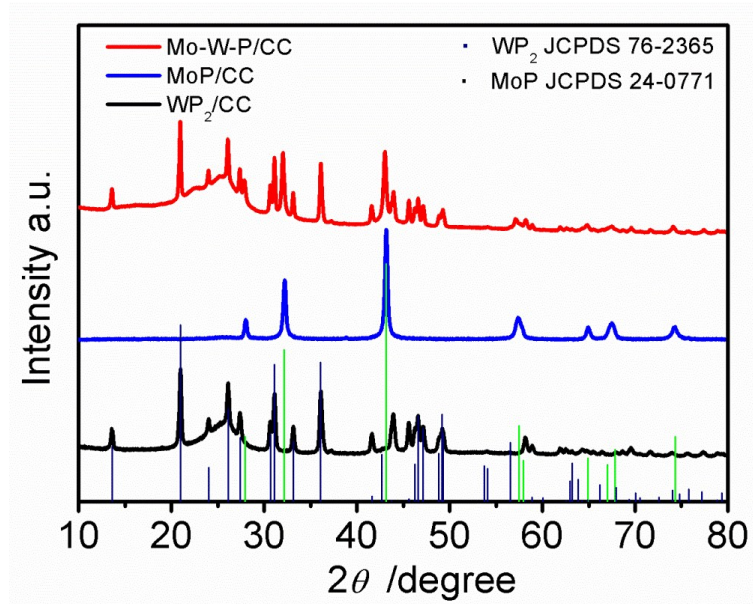


Fig. S5 The XRD patterns of Mo-W-P/CC, MoP/CC, and WP_2/CC .

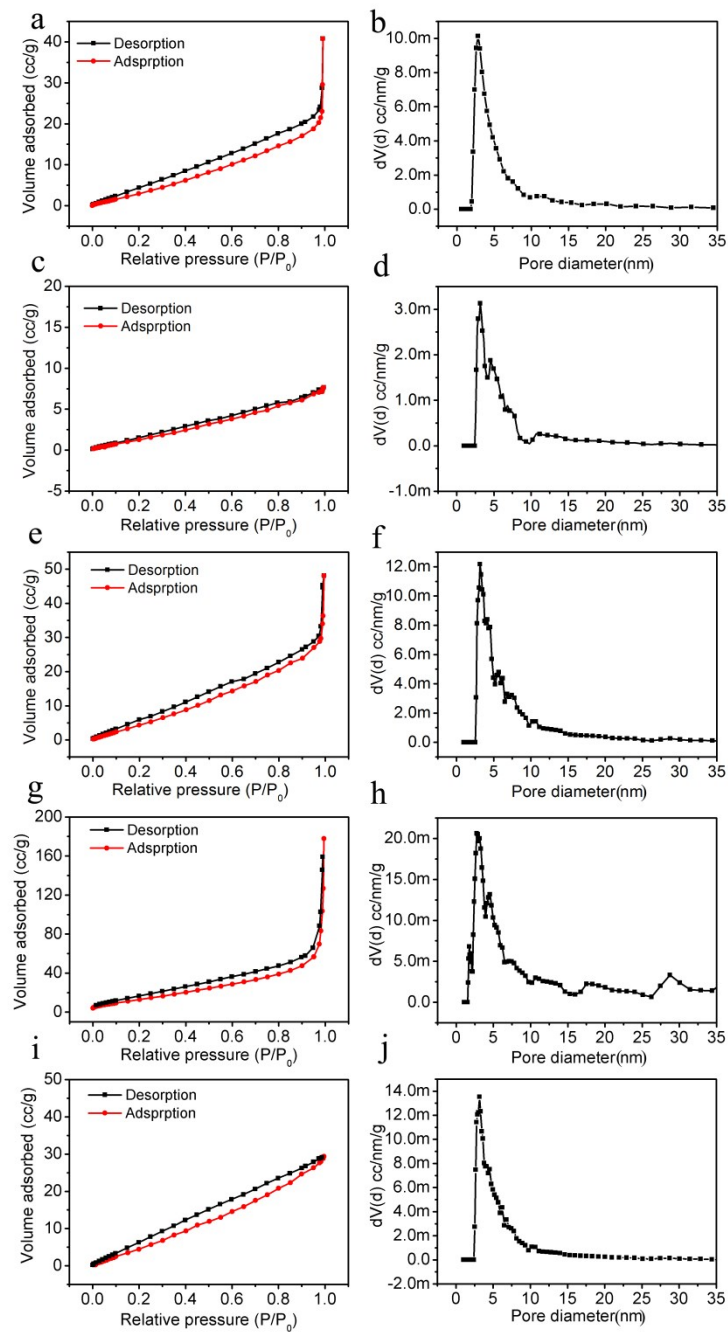


Fig. S6 (a, c, e, g, i) Nitrogen adsorption/desorption isotherm plots and (b, d, f, h, j) the BJH pore-size distribution curves of Mo-W-P/CC, MoP/CC, WP₂/CC, Pt/C/CC and CC.

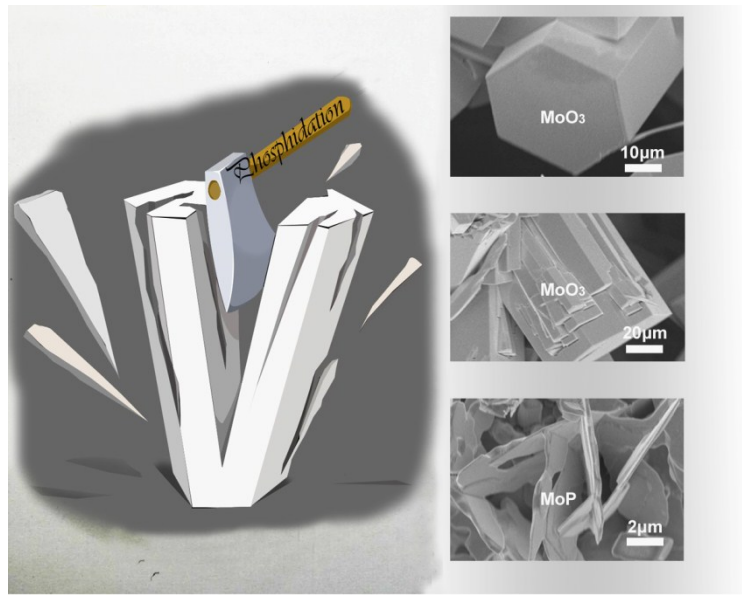


Fig. S7 Schematic illustration of the cleavage of MoO_3 nanorods to MoP nanosheets after phosphidation.

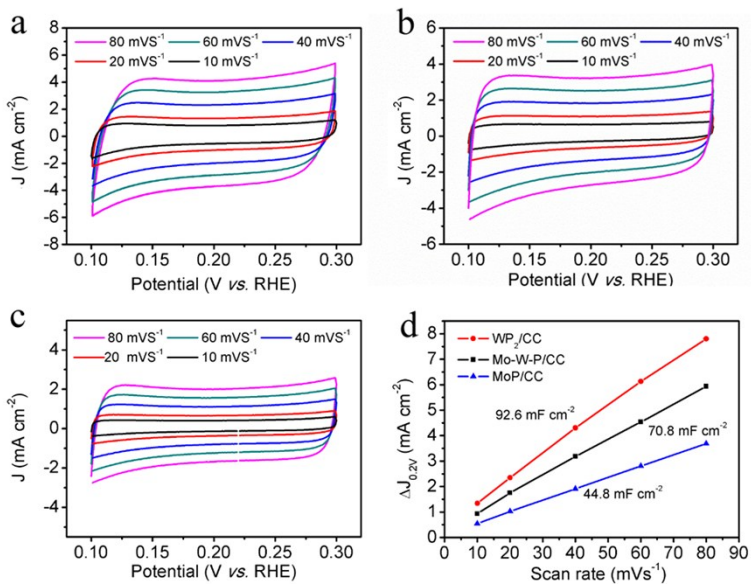
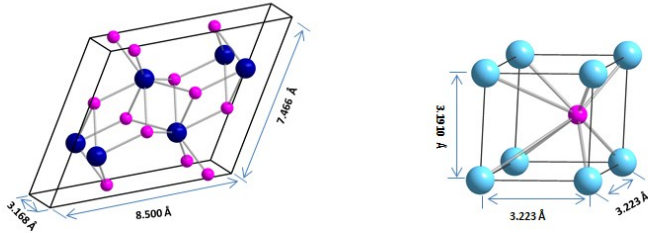


Fig. S8. Cyclic voltammograms in the region of 0.1–0.3 V vs. RHE at various scan rates and the corresponding linear fitting of the capacitive currents vs. scan rates to estimate the double layer capacitance: (a) WP_2/CC , (b) $\text{Mo-W-P}/\text{CC}$ and (c) MoP/CC ; (d) The capacitive currents were measured at 0.20 V vs. RHE plotted as a function of scan rate.



WP₂ unit cell:
Volume: 175.21 Å³
Contains: 4 W and 8 P atoms

MoP unit cell:
Volume: 28.71 Å³
Contains: 1 Mo and 1 P atom

Fig S9. WP₂ and MoP unit cells. W atoms: navy, Mo atoms: light blue and P atoms: pink. The lattice parameters from reference X-ray diffraction patterns (PDF cards No.24-0771 for MoP and 76-2365 for WP₂) are used to calculate the densities of active sites.

The specific capacitance can be converted into an electrochemically active surface area (ECSA) using the specific capacitance value for a flat standard with 1 cm² of real surface area. The specific capacitance for a flat surface is generally found to be in the range of 20-60 µF cm⁻².¹⁻⁴ In the following calculations of TOF, we assume 40 µF cm⁻² as a moderate value.

Calculated electrochemical active surface area:

$$A_{\text{ECSA}} = \frac{\text{specific capacitance}}{40 \mu\text{F cm}^{-2} \text{ per cm}^2_{\text{ECSA}}}$$

Turnover Frequency Calculations.

To calculate the persite turnover frequency (TOF), we used the following formula:²

$$\text{TOF} = \frac{\text{number of total hydrogen turnovers/cm}^2 \text{ of geometric area}}{\text{number of active sites/cm}^2 \text{ of geometric area}}$$

The total number of hydrogen turnovers was calculated from the current density according to:⁵

$$\begin{aligned} \text{no. of H}_2 &= \left(j \frac{\text{mA}}{\text{cm}^2} \right) \left(\frac{1 \text{Cs}^{-1}}{1000 \text{mA}} \right) \left(\frac{1 \text{mol of e}^-}{96485.3 \text{ C}} \right) \left(\frac{1 \text{mol of H}_2}{2 \text{mol of e}^-} \right) \left(\frac{6.022 \times 10^{22} \text{ H}_2 \text{ molecules}}{1 \text{mol H}_2} \right) \\ &= 3.12 \times 10^{15} \frac{\text{H}_2/\text{s}}{\text{cm}^2} \text{ per } \frac{\text{mA}}{\text{cm}^2} \end{aligned}$$

Active sites per real surface area:

$$\text{Active sites}_{\text{MoP}} = \left(\frac{2 \text{ atom/unit cell}}{28.71 \text{ Å}^3 / \text{unit cell}} \right)^{\frac{2}{3}} = 1.693 \times 10^{15} \times \text{atoms cm}^{-2}_{\text{real}}$$

$$\text{Active sites}_{\text{WP}_2} = \left(\frac{12 \text{ atom/unit cell}}{175.2 \text{ Å}^3 / \text{unit cell}} \right)^{\frac{2}{3}} = 1.674 \times 10^{15} \times \text{atoms cm}^{-2}_{\text{real}}$$

Since the exact cell parameters of Mo-W-P is not known, and the surface sites of MoP and WP₂ are similar, therefore the average value of MoP and WP₂ was taken to calculate the surface site density hybrid nanosheets. Finally, the plot of current density can be converted into a TOF plot according to:

$$\text{TOF} = \frac{(3.12 \times 10^{15} \frac{\text{H}_2/\text{s}}{\text{cm}^2} \text{ per } \frac{\text{mA}}{\text{cm}^2})}{\text{surface sites} \times A_{\text{ECSA}}} \times |j|$$

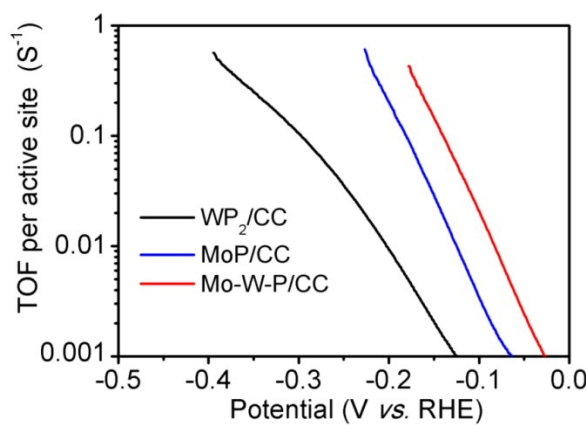


Fig. S10. TOF curves of WP₂/CC, MoP/CC and Mo-W-P.

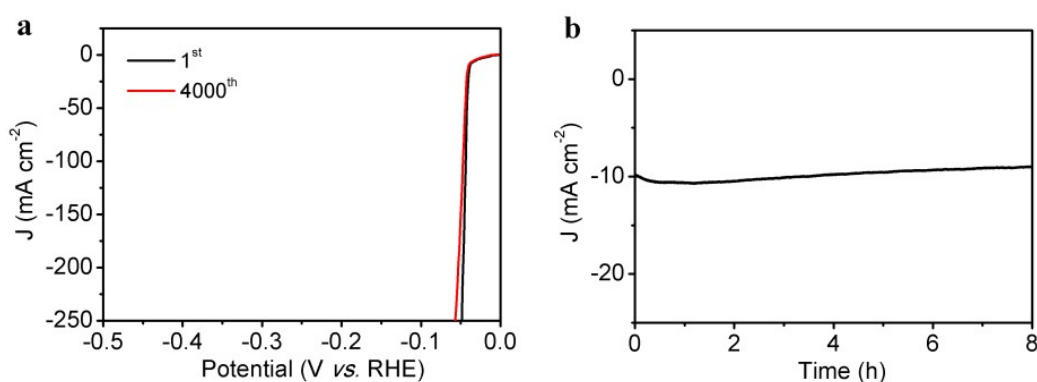


Fig. S11 (a) Stability of Pt/C/CC in H₂SO₄ solution (0.5 M) with a scan rate of 100 mVs⁻¹ before and after 4000 cycles between -0.2 and +0.2 V (RHE); (b) Time dependence of catalytic current density during electrolysis for Pt/C/CC at -35 mV (RHE).

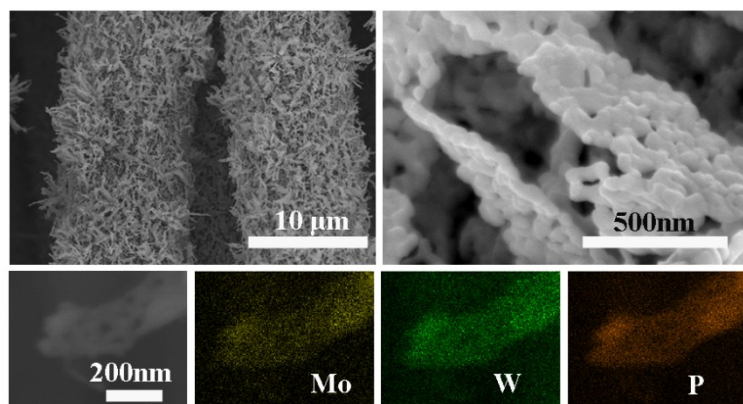


Fig. S12 (a-b) SEM images and EDX elemental mapping images (c-f) of Mo-W-P/CC after 8h stability measurement at -100 mV (RHE).

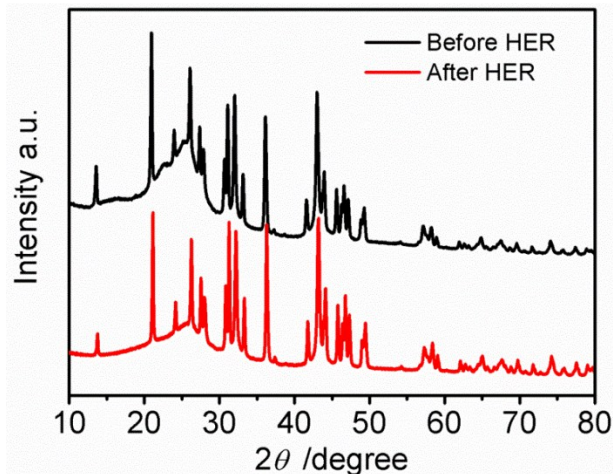


Fig. S13 XRD patterns for Mo-W-P nanosheets before and after 8h stability measurement at -100 mV (RHE).

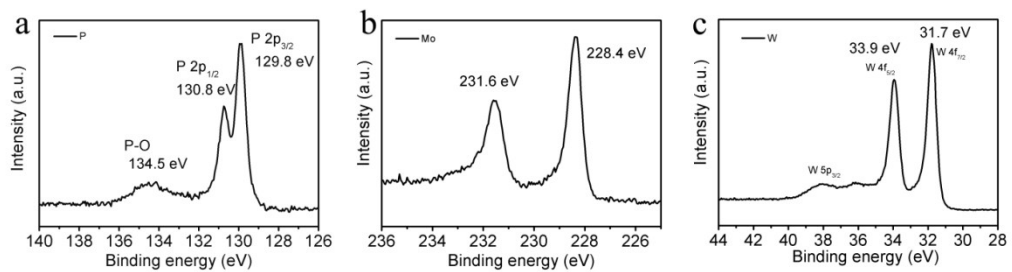


Fig. S14 XPS spectra for Mo-W-P nanosheets after 8h stability measurement at -100 mV (RHE).

Table S1. Structural information derived from the Rietveld analysis of the XRD patterns of the Mo-W-O/CC.

Phase	Space group	Phase abundance [wt%]	Cell parameters [Å]	Particle size [nm]
Graphite	$P6_3/mmc$	51±1	$a = 2.512 \pm 0.004$ $c = 7.153 \pm 0.002$	—
$\text{Mo}_{0.62}\text{W}_{0.38}\text{O}_3$ solid solution	$P2_1/m$	31±3	$a = 3.883 \pm 0.012$ $b = 3.707 \pm 0.008$ $c = 7.149 \pm 0.016$ $\alpha = 96.1^\circ \pm 0.7$	78±4
$\text{W}_{0.55}\text{Mo}_{0.45}\text{O}_3$ solid solution	$P6_3/mcm$	17±5	$a = 7.412 \pm 0.003$ $c = 7.683 \pm 0.003$	57±6

Table S2. Chemical composition of the Mo-W-P electrocatalyst.

Catalyst	Mo (at%)	W (at%)	P (at%)
Mo-W-P	20.98	12.43	66.59

The result reveals that the mole ratio Mo:W:P is 1.68:1:5.35, determined by ICP-AES spectroscopy.

Table S3 Comparison of HER performance in acid media for Mo-W-P/CC and MoP/CC with other MoP and WP₂ based HER electrocatalysts.

Catalyst	Tafel slope 0.5 M H ₂ SO ₄ mV dec ⁻¹	Current density (j , mA cm ⁻²)	Overpotential at the corresponding j (mV)	exchange current density (j_0 , mA cm ⁻²)	Ref.
Mo-W-P /CC	52	100	138	0.288	This work
MoP particles	60	10	246	0.004	Chem. Commun. 2014, 50, 11683
MoP flakes	71.8	20	155	—	AJAC 2014, 05, 1200-1213
MoP particles	54	30	180	0.034	Energy Environ. Sci., 2014, 7, 2624-2629
Amorphous MoP	45	10 20 2	90 105 84	0.12	Chem. Mater. 2014, 26, 4826-4831
MoP-CA2	54	10 100	125 200	0.086	Adv. Mater. 2014, 26, 5702-5707
MoP	50	10	117	0.05	Angew. Chem. Int. Ed. 2014, 53, 14433-14437
Commercial MoP	50	10	150	0.01	J. Mater. Chem. A, 2015, 3,4368-4373
MoP nanosheet/C F	56.4	10 2	200 101	—	Appl. Catal. B: Environ. 2015, 164, 144-150
WP ₂ NRs	52	10 2	148 101	0.013	J. Power Sources 2015, 278, 540-545
WP ₂ Sub-Particle	57	10 2	161 115	0.017	ACS Catal. 2015, 5, 145-149

Table S4. Peak attributions, angular positions, interplanar distances, relative intensities and h k l indexing derived from the Rietveld analysis of the XRD patterns for the Mo-W-O/CC.

Attribution	2 Theta	Interplanar distance (Å)	I/I _{max}	h	k	l
Mo _{0.62} W _{0.38} O ₃	12.44	7.1085	51	0	0	1
W _{0.55} Mo _{0.45} O ₃	13.79	6.4190	66	1	0	0
Mo _{0.62} W _{0.38} O ₃	23.02	3.8610	31	1	0	0
W _{0.55} Mo _{0.45} O ₃	23.14	3.8415	48	0	0	2
W _{0.55} Mo _{0.45} O ₃	23.99	3.7060	20	1	1	0
Graphite	24.89	3.5750	100	0	0	2
Mo _{0.62} W _{0.38} O ₃	25.03	3.5550	100	-1	0	1
Mo _{0.62} W _{0.38} O ₃	25.03	3.5543	63	0	0	2
W _{0.55} Mo _{0.45} O ₃	27.03	3.2963	20	1	0	2
Mo _{0.62} W _{0.38} O ₃	27.41	3.2510	37	1	0	1
W _{0.55} Mo _{0.45} O ₃	27.77	3.2095	100	2	0	0
W _{0.55} Mo _{0.45} O ₃	33.58	2.6672	11	1	1	2
Mo _{0.62} W _{0.38} O ₃	36.09	2.4866	16	1	0	2
W _{0.55} Mo _{0.45} O ₃	36.45	2.4630	75	2	0	2
W _{0.55} Mo _{0.45} O ₃	37.02	2.4261	4	1	2	0
Mo _{0.62} W _{0.38} O ₃	37.94	2.3695	41	0	0	3
Graphite	41.51	2.1737	3	0	1	0
W _{0.55} Mo _{0.45} O ₃	42.20	2.1397	4	3	0	0
Mo _{0.62} W _{0.38} O ₃	42.56	2.1226	12	-1	0	3
Graphite	43.48	2.0797	16	0	1	1
W _{0.55} Mo _{0.45} O ₃	44.11	2.0513	8	-1	3	2
Mo _{0.62} W _{0.38} O ₃	47.03	1.9305	5	2	0	0
W _{0.55} Mo _{0.45} O ₃	47.29	1.9208	10	0	0	4
Mo _{0.62} W _{0.38} O ₃	47.43	1.9152	20	-2	0	1
W _{0.55} Mo _{0.45} O ₃	48.67	1.8693	6	3	0	2
Graphite	49.01	1.8573	3	0	1	2
Mo _{0.62} W _{0.38} O ₃	49.11	1.8535	31	0	2	0
W _{0.55} Mo _{0.45} O ₃	49.13	1.8530	23	2	2	0
W _{0.55} Mo _{0.45} O ₃	49.49	1.8401	5	1	0	4
Mo _{0.62} W _{0.38} O ₃	50.23	1.8149	12	2	0	1
Mo _{0.62} W _{0.38} O ₃	50.87	1.7935	3	0	-2	1
Graphite	51.05	1.7875	7	0	0	4
W _{0.55} Mo _{0.45} O ₃	51.28	1.7803	6	1	3	0
Mo _{0.62} W _{0.38} O ₃	51.36	1.7775	11	-2	0	2
W _{0.55} Mo _{0.45} O ₃	53.71	1.7053	4	1	1	4
Mo _{0.62} W _{0.38} O ₃	54.45	1.6837	7	-1	0	4
Mo _{0.62} W _{0.38} O ₃	54.90	1.6709	5	-1	2	0
W _{0.55} Mo _{0.45} O ₃	54.97	1.6690	58	2	2	2
W _{0.55} Mo _{0.45} O ₃	55.73	1.6481	30	2	0	4
Mo _{0.62} W _{0.38} O ₃	55.89	1.6435	20	-1	2	1

$\text{Mo}_{0.62}\text{W}_{0.38}\text{O}_3$	55.90	1.6435	13	0	-2	2
$\text{Mo}_{0.62}\text{W}_{0.38}\text{O}_3$	56.57	1.6255	1	2	0	2
$\text{W}_{0.55}\text{Mo}_{0.45}\text{O}_3$	56.96	1.6153	6	1	3	2
$\text{Mo}_{0.62}\text{W}_{0.38}\text{O}_3$	57.16	1.6102	9	1	-2	1
Graphite	57.32	1.6061	5	0	1	3
$\text{W}_{0.55}\text{Mo}_{0.45}\text{O}_3$	57.37	1.6047	14	4	0	0
$\text{Mo}_{0.62}\text{W}_{0.38}\text{O}_3$	59.48	1.5529	8	1	0	4

Table S5. Peak attributions, angular positions, interplanar distances, relative intensities and $h\ k\ l$ indexing derived from the Rietveld analysis of the XRD patterns for the Mo-W-P/CC.

Attribution	2 Theta	Interplanar distance (Å)	I/I_{max}	h	k	l
$\text{W}_{0.59}\text{Mo}_{0.41}\text{P}_2$	13.59	6.5105	28	0	0	1
$\text{W}_{0.59}\text{Mo}_{0.41}\text{P}_2$	20.96	4.2356	100	-2	0	1
$\text{W}_{0.59}\text{Mo}_{0.41}\text{P}_2$	23.99	3.7067	20	-4	0	3
Graphite	24.84	3.582	100	0	0	2
$\text{W}_{0.59}\text{Mo}_{0.41}\text{P}_2$	26.09	3.4123	57	-1	1	1
$\text{W}_{0.59}\text{Mo}_{0.41}\text{P}_2$	27.38	3.2553	42	-2	0	3
$\text{Mo}_{0.84}\text{W}_{0.16}\text{P}$	27.91	3.194	18	0	0	1
$\text{Mo}_{0.84}\text{W}_{0.16}\text{P}$	30.67	2.9124	41	-1	1	2
$\text{W}_{0.59}\text{Mo}_{0.41}\text{P}_2$	31.11	2.8727	90	2	0	0
$\text{W}_{0.59}\text{Mo}_{0.41}\text{P}_2$	32.03	2.7921	64	1	0	0
$\text{W}_{0.59}\text{Mo}_{0.41}\text{P}_2$	33.13	2.7017	41	0	0	3
$\text{W}_{0.59}\text{Mo}_{0.41}\text{P}_2$	36.1	2.486	85	-2	0	2
$\text{W}_{0.59}\text{Mo}_{0.41}\text{P}_2$	36.26	2.4753	15	-4	0	4
$\text{W}_{0.59}\text{Mo}_{0.41}\text{P}_2$	37.22	2.4138	3	-4	-2	1
$\text{W}_{0.59}\text{Mo}_{0.41}\text{P}_2$	41.58	2.1702	30	-3	-1	1
Graphite	42.32	2.1339	3	1	0	0
$\text{W}_{0.59}\text{Mo}_{0.41}\text{P}_2$	42.97	2.103	1	-4	-2	3
$\text{Mo}_{0.84}\text{W}_{0.16}\text{P}$	42.99	2.1021	100	1	0	1
$\text{W}_{0.59}\text{Mo}_{0.41}\text{P}_2$	43.7	2.0697	24	2	0	2
$\text{W}_{0.59}\text{Mo}_{0.41}\text{P}_2$	43.94	2.0588	57	1	1	0
Graphite	44.25	2.0451	14	1	0	1
$\text{W}_{0.59}\text{Mo}_{0.41}\text{P}_2$	45.58	1.9885	50	2	0	1
$\text{W}_{0.59}\text{Mo}_{0.41}\text{P}_2$	46.22	1.9625	32	-4	0	2
$\text{W}_{0.59}\text{Mo}_{0.41}\text{P}_2$	46.58	1.9482	59	0	0	2
$\text{W}_{0.59}\text{Mo}_{0.41}\text{P}_2$	47.12	1.9271	47	1	1	1
$\text{W}_{0.59}\text{Mo}_{0.41}\text{P}_2$	48.81	1.8643	25	-3	-1	2
$\text{W}_{0.59}\text{Mo}_{0.41}\text{P}_2$	49.12	1.8534	19	3	1	0
$\text{W}_{0.59}\text{Mo}_{0.41}\text{P}_2$	49.28	1.8476	29	-4	0	1
Graphite	49.69	1.8332	3	1	0	2

Graphite	50.95	1.791	7	0	0	4
$W_{0.59}Mo_{0.41}P_2$	53.68	1.7061	1	5	1	1
$W_{0.59}Mo_{0.41}P_2$	54.05	1.6952	4	1	1	4
$W_{0.59}Mo_{0.41}P_2$	56.49	1.6276	3	0	2	3
$Mo_{0.84}W_{0.16}P$	57.09	1.612	26	1	1	0
$Mo_{0.84}W_{0.16}P$	57.68	1.597	8	0	0	2
Graphite	57.91	1.5912	5	1	0	3
$W_{0.59}Mo_{0.41}P_2$	57.99	1.5891	5	4	0	2
$W_{0.59}Mo_{0.41}P_2$	58.08	1.5868	10	-5	-1	2
$W_{0.59}Mo_{0.41}P_2$	58.22	1.5835	23	1	1	2
$W_{0.59}Mo_{0.41}P_2$	58.87	1.5675	16	-2	0	4
$W_{0.59}Mo_{0.41}P_2$	59.43	1.554	1	4	2	0

Reference:

- 1 D. C. Grahame, *Chem. Rev.*, 1947, **41**, 441-501.
- 2 R. Kötz and M. Carlen, *Electrochim. Acta*, 2000, **45**, 2483-2498.
- 3 B. E. Conway and B. V. Tilak, *Electrochim. Acta*, 2002, **47**, 3571-3594.
- 4 J. D. Benck, Z. B. Chen, L. Y. Kuritzky, A. J. Forman and T. F. Jaramillo, *ACS Catal.*, 2012, **2**, 1916-1923.
- 5 J. Kibsgaard and T. F. Jaramillo, *Angew.Chem. Int. Ed.*, 2014, **53**, 14433-14437.

Supplementary Movie

This movie shows Mo-W-P hybrid nanosheets on carbon cloth catalyst operated at a large cathodic current density of 100 mA cm^{-2} to drive HER. Generated hydrogen gas is efficiently released from the electrode.